MAJOR ARTICLE

Opposing Roles of Membrane and Soluble Forms of the Receptor for Advanced Glycation End Products in Primary Respiratory Syncytial Virus Infection

Allison L. Miller,[1] Gary P. Sims,[1] Yambasu A. Brewah,[1] Marlon C. Rebelatto,[2] Jennifer Kearley,[1] Ebony Benjamin,[3] Ashley E. Keller,[1] Philip Brohawn,[4] Ronald Herbst,[1] Anthony J. Coyle,[5] Alison A. Humbles,[1,a] and Roland Kolbeck[1,a]

[1]Departments of Respiratory, Inflammation and Autoimmunity, [2]Translational Sciences—Experimental Pathology, [3]Infectious Diseases and Vaccines, and [4]Translational Sciences—Pharmacogenomics, MedImmune, LLC, Gaithersburg, Maryland; and [5]Global Therapeutic Innovation, Pfizer, Cambridge, Massachusetts

Respiratory syncytial virus (RSV), a common respiratory pathogen in infants and the older population, causes pulmonary inflammation and airway occlusion that leads to impairment of lung function. Here, we have established a role for receptor for advanced glycation end products (RAGE) in RSV infection. RAGE-deficient (*ager*$^{-/-}$) mice were protected from RSV-induced weight loss and inflammation. This protection correlated with an early increase in type I interferons, later decreases in proinflammatory cytokines, and a reduction in viral load. To assess the contribution of soluble RAGE (sRAGE) to RSV-induced disease, wild-type and *ager*$^{-/-}$ mice were given doses of sRAGE following RSV infection. Of interest, sRAGE treatment prevented RSV-induced weight loss and neutrophilic inflammation to a degree similar to that observed in *ager*$^{-/-}$ mice. Our work further elucidates the roles of RAGE in the pathogenesis of respiratory infections and highlights the opposing roles of membrane and sRAGE in modulating the host response to RSV infection.

Respiratory syncytial virus (RSV)–induced disease is characterized by inflammation, epithelial cell necrosis, and mucus overproduction that occludes the small airways of infants, leading to hypoxia and wheezing in acute disease, and in some cases, wheezing throughout childhood [1, 2]. In addition to being detrimental to very young individuals, RSV also poses a significant threat to the older population [3]. Recently, a new at-risk population for RSV infection was identified: patients with chronic obstructive pulmonary disease (COPD). The incidence of COPD is increasing, and it is predicted to be the third leading cause of death worldwide by 2030 [4]. RSV has been identified as a component of both stable and acute exacerbations of COPD (AECOPD) [5–11]. Moreover, the persistence of RSV in stable COPD has been associated with inflammation and a decrease in the forced expiratory volume in 1 second (FEV1) [11]. These data suggest that a treatment that is effective at limiting RSV pathogenesis may be a valid approach to limiting RSV-induced disease and AECOPD.

Receptor for advanced glycation end products (RAGE) can exist as a transmembrane or soluble protein [12] and binds to a variety of ligands that are released during cellular damage or stress, including advanced glycation end products, High Mobility Group Box Chromosomal Protein 1 (HMGB-1), DNA, several S100 family members, and β-amyloid [13]. RAGE is

Received 10 March 2011; accepted 7 June 2011; electronically published 18 January 2012.

Presented in part: Second International Congress on Exacerbations of Airway Disease, 17–19 April 2010, Miami Beach, Florida; American Thoracic Society Annual Meeting, 14–19 May 2010, New Orleans, Louisiana; Keystone Symposium "Innate Immunity: Mechanisms Linking with Adaptive Immunity," 7–12 June 2010, Dublin, Ireland; Toll 2011 Meeting, 4–7 May 2011, Verona, Italy.

[a]A. A. H. and R. K. contributed equally to this work.

Correspondence: Alison Humbles, PhD, MedImmune, LLC, 1 MedImmune Way, Gaithersburg, MD 20878 (humblesa@medimmune.com).

The Journal of Infectious Diseases 2012;205:1311–20

DOI: 10.1093/infdis/jir826

reported to be highly expressed by types I and II alveolar epithelial cells in healthy lung tissue from humans and mice, respectively [14, 15]. Expression has also been reported on vascular endothelial cells, neutrophils, macrophages, and dendritic cells. In studies using *ager*$^{-/-}$ mice, RAGE has been shown to play detrimental roles in response to both influenza A [16] and *Streptococcus pneumonia* [17], two known mediators of AECOPD. In this study, we examined the role of RAGE in RSV infection with the hypothesis that RAGE may contribute to the ability of RSV to cause AECOPD.

Here, we demonstrate that endogenous RAGE serves to exacerbate RSV-induced disease. Specifically, *ager*$^{-/-}$mice were markedly protected from RSV-induced weight loss and lung inflammation. This phenotype was accompanied by small but significant decreases in viral RNA and proteins, compared with wild-type (WT) controls. The protective effects of RAGE deficiency were associated with an early increase in the type I interferons (IFN-I) and a decrease in proinflammatory cytokines at 5 days after infection. Levels of soluble RAGE (sRAGE) were elevated in the bronchoalveolar lavage fluid (BALF) of WT mice at 5 days after infection, a time point that coincided with weight loss and inflammation; however, our data suggest that sRAGE is anti-inflammatory and serves to self-limit the inflammatory response. Our findings highlight the opposing functions of membrane and sRAGE and suggest that modulation of RAGE, either by complete removal of the protein, or by administration of sRAGE, has the potential to dampen RSV-induced illness and inflammation without compromising host defense.

MATERIALS AND METHODS

Mice

ager (Gene product, RAGE) knockout mice were generated by Taconic Artemis Pharmaceuticals by means of the targeting strategy detailed in Figure 1. C57/B6 and *ager*$^{-/-}$ mice were housed under specific pathogen-free conditions at Taconic Farms and MedImmune. All experiments were approved by MedImmune's internal Institutional Animal Use and Care Committee.

RSV Propagation

RSV A2 strain virus was propagated in Hep2 cells. Cells were infected with virus at a multiplicity of infection of 0.1 plaque-forming units/cell. At 4–5 days after infection, viable virion particles were harvested from infected cultures by performing multiple freeze-thaw cycles on the infected cell pellet. Suspension was clarified by centrifugation, and supernatant containing infectious virions was stored at −80°C.

RSV Infection and Necropsy

Mice were anesthetized with isofluorane before intranasal inoculation with 50 μL of RSV (6.78×10^6 plaque-forming units) or media. Mice were monitored daily for weight loss. At the time of necropsy, we collected blood, BALF, and lung tissue samples (for RNA, protein, lung dispersions, and histological examination). An in-house preparation of sRAGE-huFc or human immunoglobulin (Ig) G Fc fragment (Jackson Immunoresearch) was administered intranasally in 50-μg doses.

Determination of Viral Load

A plaque assay, genome-transcript analysis, and enzyme-linked immunosorbent assay (ELISA) were used to determine viral load in RSV-infected WT and *ager*$^{-/-}$ mice. Serial dilutions of lung or nasal turbinate homogenates were used to determine lung viral titers with use of plaque assay by titration on confluent Hep-2 or Vero cells. On day 5–7 after infection, cell monolayers were fixed and were immunostained with anti-RSV antibodies to identify plaques [18]. We used real-time polymerase chain reaction primer-probe sets for RSV N, RSV SH-G, and RSV NS1 to assess viral genome and transcript, viral genome, and viral transcript, respectively. Analysis of RSV proteins in lung tissue and BALF samples was done using an RSV ELISA, as described elsewhere [19].

RNA Isolation and Gene Expression Analyses

Lung tissue for RNA analysis was incubated in RNAlater (Ambion) and was maintained at 4°C overnight, after which the RNAlater was removed and the tissues were frozen at −80°C. RNA was isolated from homogenized tissue using the RNeasy kit from Qiagen. RNA was reverse-transcribed using the Superscript III RT system (Invitrogen). Relative cytokine-chemokine transcript expression was assessed using the Fluidigm Biomark Dynamic array loaded with probes for transcripts of interest.

Quantification of Cytokine and Chemokine Levels

Lung tissue was homogenized in the presence of Complete protease inhibitors (Roche), and cytokines were measured using an MSD platform (MesoScale Diagnostics). RAGE levels were assessed using a duoset purchased from R&D Systems. Myeloperoxidase (MPO) was assessed using a kit from Cell Sciences. IFN-I levels were assessed using kits from PBL Interferon Source.

Lung Dispersions and Flow Cytometry Fluorescence Activated Cell Sorting

Lung tissue was processed into a single cell suspension after incubation with a solution of 0.22 Wunsch U/mL of Liberase and 0.01 U/μL DNAse in RPMI (Roche). Antibodies used for staining included those against CD4, CD8, TCRβ, DX5, CD19, F4/80, Gr1, CD11c, B220, and PDCA1. All antibodies were purchased from BD Biosciences.

Histological Analyses

Lung tissue harvested for histological analyses was inflated with 10% buffered formalin before paraffin embedding and sectioning. Tissue sections were stained with hematoxylin-eosin.

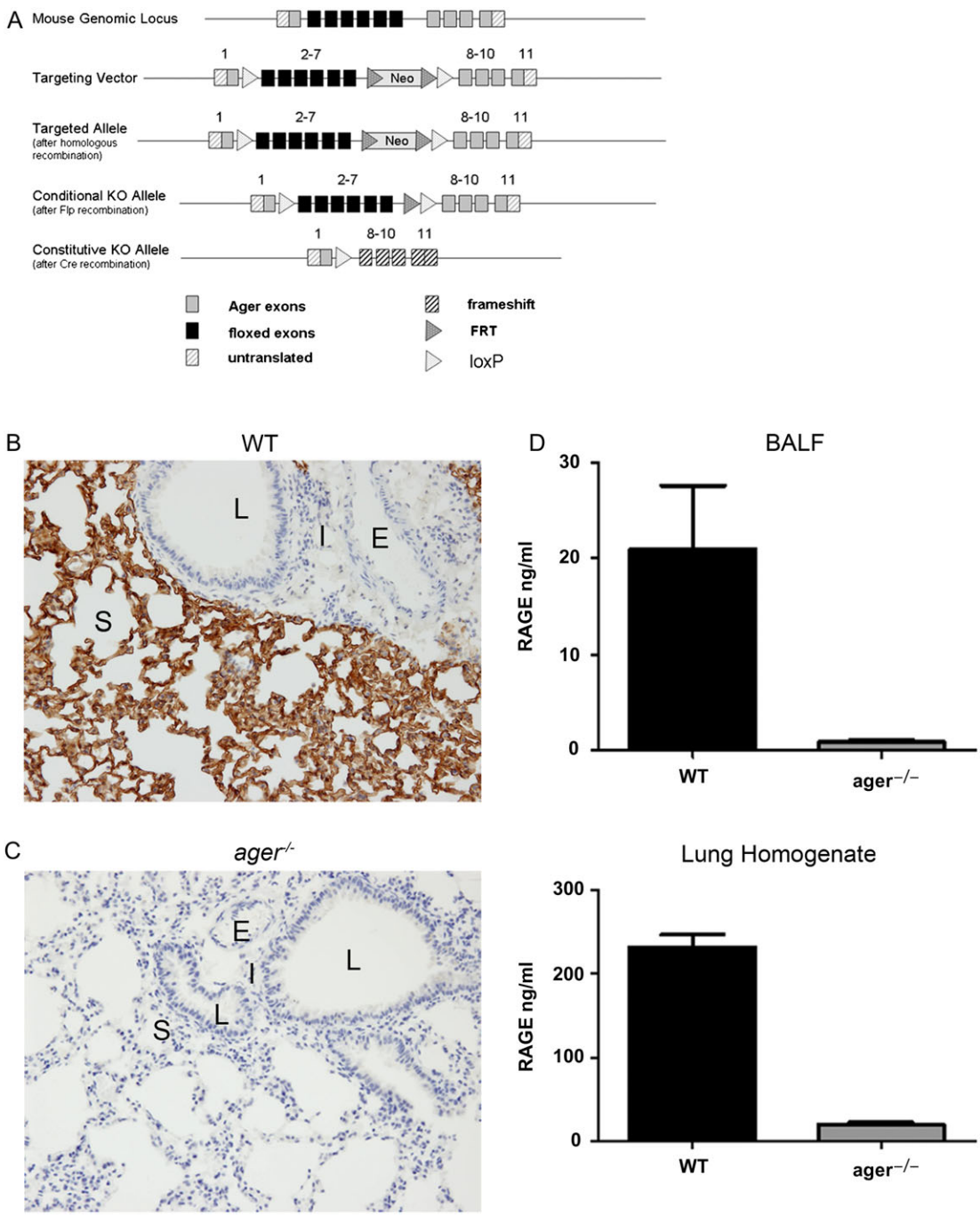

Figure 1. *A,* Receptor for advanced glycation end products (RAGE) protein is absent in *ager*$^{-/-}$ mice, generated using a targeting construct to delete exons 2–7. *B, C,* Small airways of wild-type (WT) mice (*B*) but not *ager*$^{-/-}$ mice (*C*) express RAGE protein, as indicated by red staining. *D,* Immunohistochemical results were confirmed by enzyme-linked immunosorbent assay analysis.

RESULTS

RAGE Expression in Small Airways of WT Mice

RAGE-deficient (*ager*$^{-/-}$) mice were generated using a vector that targeted exons 2–7 of *ager* for deletion (Figure 1*A*). Lungs from C57/BL6 WT and *ager*$^{-/-}$ mice were immunohistochemically stained for RAGE to identify the RAGE-expressing cells. RAGE, as indicated by red staining, was highly expressed in types I and II alveolar epithelial cells lining the small airways but not in the large airways, interstitium, or endothelium (Figure 1*B*). Of importance, no immunoreactivity for RAGE was detected in *ager*$^{-/-}$ mice

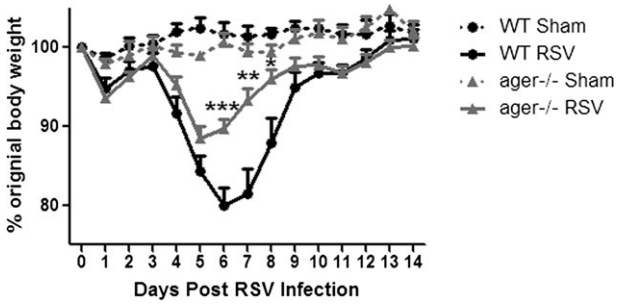

Figure 2. *ager*$^{-/-}$ mice are protected from respiratory syncytial virus (RSV)–induced weight loss. Wild-type (WT) and *ager*$^{-/-}$ mice were infected with RSV or media (sham), and weight loss was monitored over a period of 14 days. Graph represents pooled weight change data ± standard error of the mean from 2 experiments (n = 6–22). Statistically significant difference between RSV-infected WT and *ager*$^{-/-}$ mice: $*P \leq .05$, $**P \leq .01$, $***P \leq .001$.

(Figure 1*C*). Further validation by ELISA detected high basal levels of RAGE in the lung tissue (Figure 1*D*) and BALF (Figure 1*D*) from WT mice, whereas RAGE levels in *ager*$^{-/-}$ mice were undetectable or at background levels (Figure 1*D*).

Protection From RSV-Induced Weight Loss in *ager*$^{-/-}$ Mice

RSV infection causes transient weight loss in mice [20–25], and this parameter is often used to assess virus-induced illness [26, 27]. In our model, both RSV-infected WT and *ager*$^{-/-}$ mice exhibited a transient weight loss of similar magnitude at 1 day after infection. Mice recovered from this weight loss before beginning a second period of weight loss starting at 4 days after infection, relative to sham controls (Figure 2). Peak weight loss in RSV-infected WT mice (80% ± 2% of original body weight) was observed at 6 days after infection. However, this value reflects only the weight loss for mice that were monitored over the full period; 13 of the 22 RSV-infected WT mice were euthanized at 7 days after infection because of ≥25% loss of their original body weight (according to MedImmune Institutional Animal Care and Use Committee guidelines). In comparison, the degree of RSV-induced weight loss in *ager*$^{-/-}$ mice (90% ± 1% at 6 days after infection) was significantly reduced relative to WT controls. None of the *ager*$^{-/-}$ mice lost ≥25% of their original body weight.

Reduced Viral Load in Nasal Turbinates of *ager*$^{-/-}$ Mice

We next examined the viral load 4 days after infection, when peak viral titers were recovered from RSV-infected WT mice [28]. Viral titers from WT and *ager*$^{-/-}$ mice were similar, with

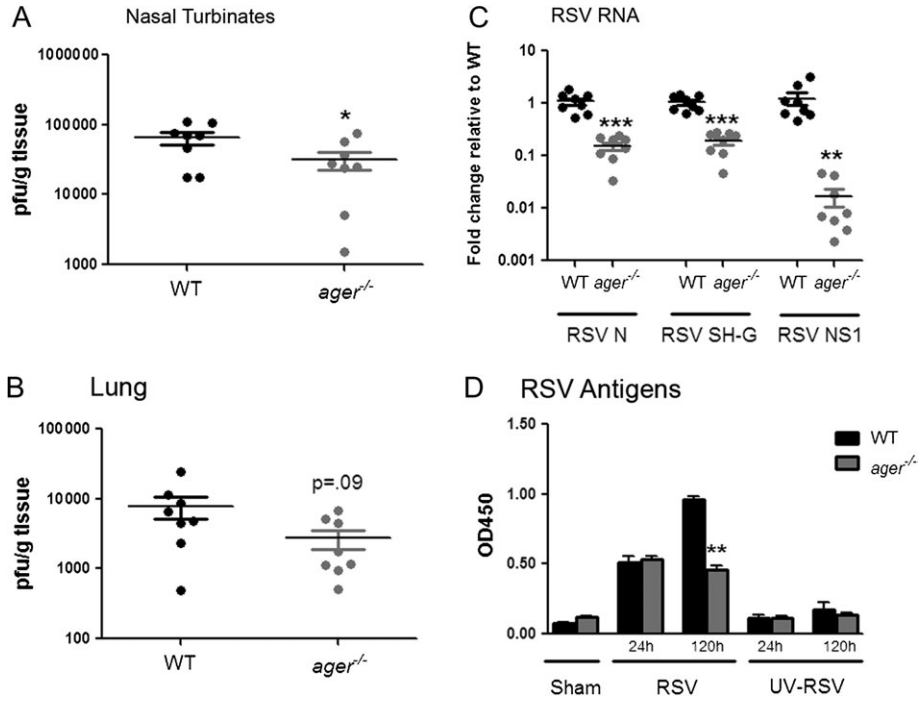

Figure 3. *ager*$^{-/-}$ mice have a reduced viral load after respiratory syncytial virus (RSV) infection. *A, B, ager*$^{-/-}$ mice had significantly fewer plaque-forming units (PFUs) per gram isolated from nasal turbinates (*A*) but not lung tissue (*B*), compared with wild-type (WT) mice. *C, ager*$^{-/-}$ mice displayed statistically significant decreases in viral genome and/or transcript RNAs. Primers for N protein, SH-G, and NS1 were designed to amplify genome and transcripts, genome only, and transcripts only, respectively. Data are plotted as fold change in RNA relative to RSV-infected WT mice. *D, ager*$^{-/-}$ mice had lower levels of viral antigens than did WT mice, as determined by enzyme-linked immunosorbent assay. All data are plotted as mean ± standard error of the mean and are representative of ≥2 separate experiments. $*P \leq .05$, $**P \leq .01$, $***P \leq .001$.

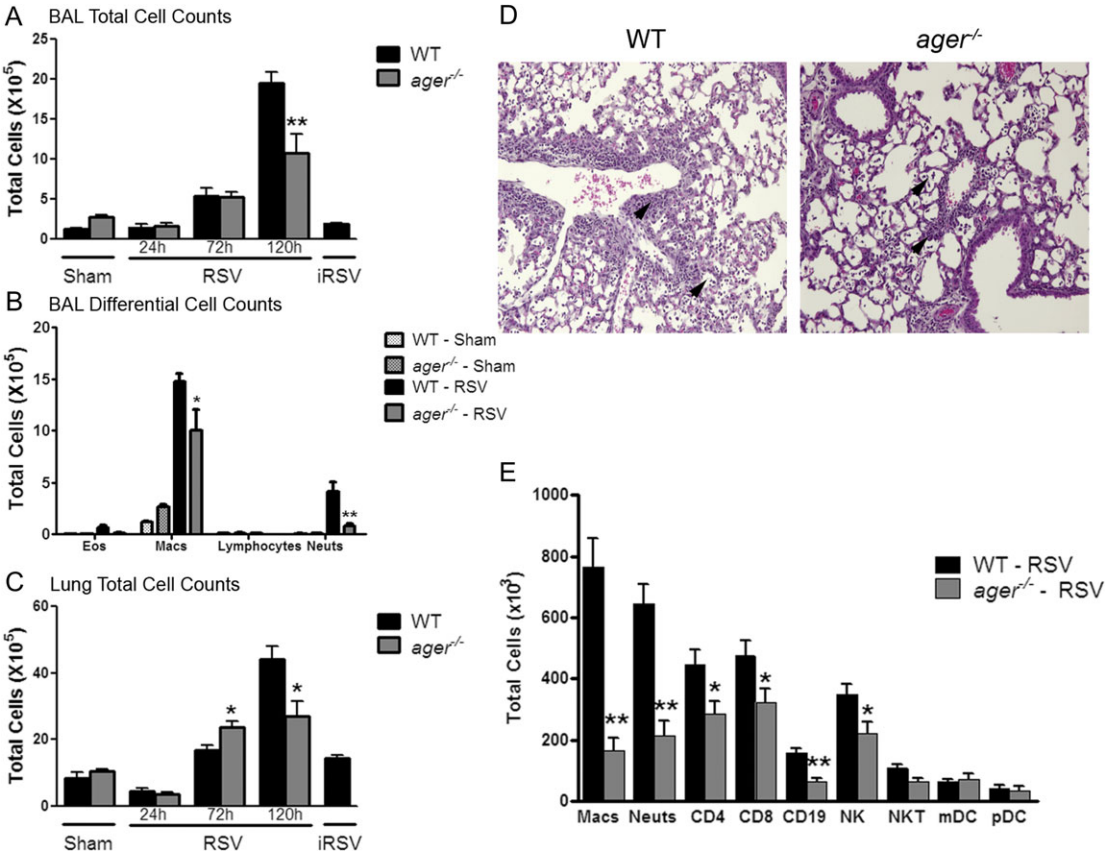

Figure 4. Respiratory syncytial virus (RSV)–induced inflammation is dampened in the absence of receptor for advanced glycation end products (RAGE). *A, B,* RSV-infected *ager*$^{-/-}$ mice have less inflammation in bronchoalveolar lavage fluid (BALF) at 120 hours after infection, relative to RSV-infected wild-type (WT) controls (*A*); specifically, there were fewer macrophages and neutrophils (*B*), as assessed by differential counts. *C, D,* RSV-infected *ager*$^{-/-}$ mice had decreased lung tissue inflammation, compared with RSV-infected WT mice, as assessed by lung digests (*C*) and histology (*D*). Arrowheads indicate airway and perivascular inflammation, both reduced in *ager*$^{-/-}$ mice at 120 hours after infection (*D*). Data in panels *A–C* are plotted as the mean ± standard error of the mean and are representative of ≥ 2 separate experiments. *E,* Flow cytometric analysis of lung digests from RSV-infected *ager*$^{-/-}$ and WT mice show that the former have decreases in many leukocyte populations relative to the latter. Plotted FACS data represent pooled data from 3 separate experiments, with 3–6 animals per experiment. *$P \leq .05$, **$P \leq .01$ (difference between RSV-infected WT and *ager*$^{-/-}$ mice at a particular time point).

a small but significant decrease in virions recovered from the nasal turbinates of *ager*$^{-/-}$ mice (Figure 3*A* and 3*B*). In addition, we observed a significant decrease in RSV RNA in *ager*$^{-/-}$ mice with use of primers for RSV N, SH-G, and NS1, which detected genome and transcript, genome only, and transcript only, respectively. The *ager*$^{-/-}$ mice had a mean of 7-fold less N protein, 5.5-fold less SH-G, and 74-fold less NS1, compared with WT mice (Figure 3*C*). Correspondingly, levels of RSV antigens in the lung were reduced significantly in the absence of RAGE (Figure 3*D*).

Dampened RSV-Induced Inflammation in the Absence of RAGE

At 5 days after infection, the total cell numbers in BALF and lung tissue were markedly reduced (~50%) in RSV-infected *ager*$^{-/-}$ mice, compared with WT controls (Figure 4*A* and 4*C*). Differential counts revealed that the reduction in total BALF inflammation was attributable to fewer infiltrating macrophages and neutrophils (Figure 4*B*). Accordingly, histological analyses showed that perivascular and peribronchial inflammation was reduced in the lungs of the *ager*$^{-/-}$ mice (Figure 4*D*). Although RSV infection in WT mice resulted in the recruitment of a variety of leukocyte populations to the lung, numbers of macrophages (F4/80^{+}/CD11b^{+}), neutrophils (Gr-1^{hi}/CD11b^{hi}), B cells (CD19^{+}), natural killer (NK) cells (DX5^{+}/TCRβ^{-}), CD4^{+} T cells, and CD8^{+} T cells were significantly reduced in the absence of RAGE (Figure 4*E*). RAGE deficiency did not alter NKT cell (DX5^{+}/TCRβ^{+}), mDC (CD11c^{hi}, CD11b^{+}, PDCA^{-}), or pDC (PDCA^{+}, Gr-1^{+}, B220^{+}) numbers in the lung after infection. Infection of mice with ultraviolet-inactivated RSV did not induce pulmonary inflammation (Figure 4*A* and 4*C*).

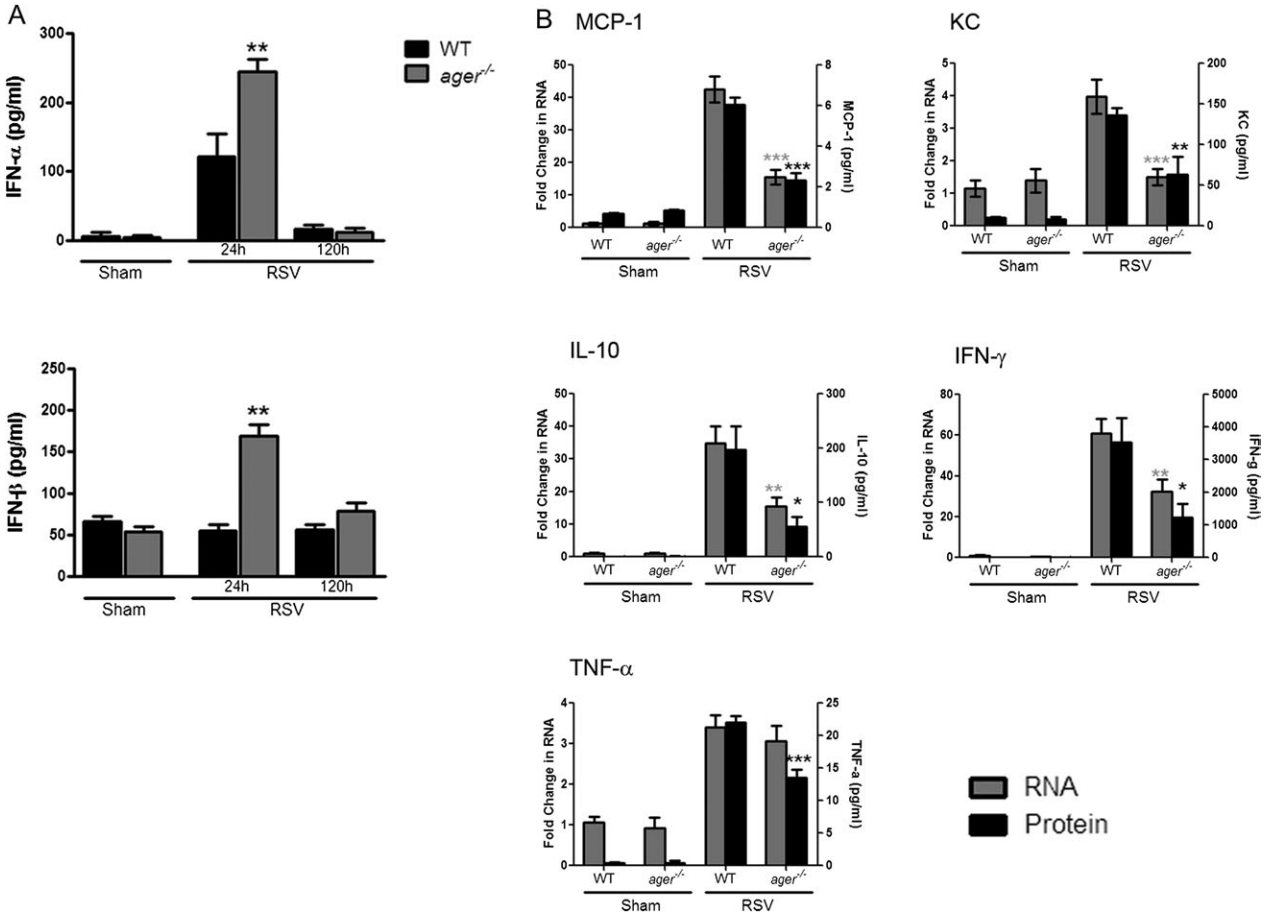

Figure 5. Respiratory syncytial virus (RSV)–infected *ager*$^{-/-}$ mice have altered cytokine and chemokine profiles. RSV-infected *ager*$^{-/-}$ mice display enhanced levels of IFN-I at 24 hours after infection (*A*) and decreased RNA (gray bars) and protein (black bars) levels for many cytokines and chemokines at 120 hours after infection (B), relative to RSV-infected wild-type (WT) controls. Fold changes in RNA were calculated relative to sham-infected WT animals. All data are plotted as mean ± standard error of the mean. Protein data are representative of ≥2 separate experiments with 4–8 animals per group. RNA data were generated by pooling samples from a variety of experiments with a total sample number of 12 per experimental group. $*P \leq .05$, $**P \leq .01$, $***P \leq .001$ (difference between RSV-infected WT and *ager*$^{-/-}$ mice at a particular time point).

Alteration of RSV-Induced Cytokine and Chemokine Induction in *ager*$^{-/-}$ Mice

To further elucidate the mechanism by which RAGE was regulating RSV-induced inflammation, we assessed cytokine and chemokine production in WT and *ager*$^{-/-}$ mice. Of interest, we observed that *ager*$^{-/-}$ mice mounted an early IFN-I response after RSV infection that was 2–3-times greater than that observed in WT mice (Figure 5*A*). However, at 5 days after infection, many of the mediators that were elevated in RSV-infected WT mice were significantly reduced in *ager*$^{-/-}$ mice, including monocyte chemoattractant protein 1 (MCP-1, CC chemokine motif ligand 2, CCL2), keratinocyte chemoattractant (KC), interleukin-10, IFN-γ, and tumor necrosis factor α (TNF-α) (Figure 5*B*).

Up-regulation of sRAGE Caused by RSV Infection

We next asked whether RSV infection had an effect on the expression of RAGE and RAGE ligands. Levels of sRAGE were significantly increased in BALF from WT mice after RSV infection and, of the time points tested, were highest at 5 days after infection (Figure 6). In contrast to published data from other infection models [16, 17], we did not observe RSV-induced increases in RAGE with use of real-time polymerase chain reaction or immunohistochemistry (data not shown). Furthermore, up-regulation of the RAGE ligands S100A8/A9 and HMGB-1 was variable and was not observed in all of the experiments conducted.

sRAGE Is Protective During RSV Infection

To determine the role of sRAGE in RSV infection, we intranasally administered sRAGE or IgG-Fc to mice at 8 hours and 3 days after infection. Administration of exogenous sRAGE elevated levels of sRAGE in the BALF of RSV-infected WT mice to 2–3-times the levels observed with RSV infection alone (Figure 7*A*). It was surprising that reconstitution of *ager*$^{-/-}$ mice with sRAGE did not dramatically alter the course

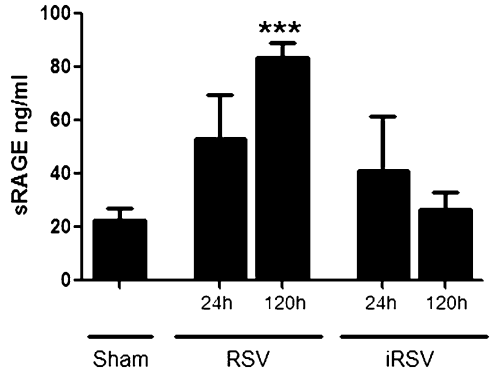

Figure 6. Soluble receptor for advanced glycation end products (sRAGE) is up-regulated during respiratory syncytial virus (RSV) infection. Levels of sRAGE in the bronchoalveolar lavage fluid (BALF) were significantly increased at 120 hours after infection with RSV. Representative data are shown, with 5–8 mice per group. $*P \leq .05$ (significant increase in sRAGE compared with sham-infected animals).

of RSV-induced disease (Figure 7*C*). However, treatment of RSV-infected WT mice with sRAGE conferred protection from RSV-induced weight loss to a degree similar to RAGE deficiency (Figure 7*B*). Furthermore, sRAGE administration markedly reduced total cell counts in BALF from WT mice (Figure 7*D*) and neutrophilic airway inflammation in RSV-infected WT mice and *ager*$^{-/-}$ mice, as assessed by differential cell counts and levels of myeloperoxidase in the BALF (Figure 7*E* and 7*F*). sRAGE alone or in the context of RSV infection did not alter levels of proinflammatory cytokines, including IFN-I and tumor necrosis factor α, in BALF or lung tissue (data not shown).

DISCUSSION

Viral and bacterial infections in the airways of infants or in the context of a lung with COPD can result in an amplification of the host response that leads to severe lung damage, airflow obstruction, and increased mortality. RAGE is highly expressed in the lungs, and there is recent literature suggesting that RAGE deficiency is protective in mouse models of infection, including cecal ligation puncture sepsis [29, 30], pulmonary influenza A [16], and *Streptococcus pneumoniae* infection [17]. In the latter 2 models, which used pathogens associated with AECOPD, a RAGE deficiency enhanced survival without compromising pathogen clearance. In fact, the absence of RAGE led to increased killing of *S. pneumoniae* [17] and to increased clearance of influenza A [16].

Although the aforementioned studies revealed a clear role for RAGE in mediating mortality after infection, the effect of RAGE on pathogen-induced inflammation was not carefully addressed. Thus, we chose to examine the role of RAGE in the context of RSV-induced inflammation. We report here that the absence of RAGE markedly protected against RSV-induced illness and airway and lung inflammation. Our results support the previous findings that RSV-induced weight loss is related to magnitude of the CD8$^+$ T-cell response [26, 31]. However, although total CD8$^+$ T-cell counts were decreased in lungs from RSV-infected *ager*$^{-/-}$ mice, antigen-specific CD8$^+$ T cell counts were not (data not shown). It should be noted that a role for endothelial RAGE in mediating vascular leukocyte adhesion has been established [17, 29, 32, 33]; however, we were unable to demonstrate an underlying defect in leukocyte recruitment to the lungs in *ager*$^{-/-}$ mice. First, we did not observe RAGE expression on murine lung endothelium either before (Figure 1*A*) or after RSV infection (data not shown). Second, KC- or macrophage inflammatory protein-1α–induced pulmonary inflammation was similar in WT and *ager*$^{-/-}$ mice (data not shown), showing that chemokine-mediated leukocyte recruitment was intact in *ager*$^{-/-}$ mice.

At 8 and 24 hours after infection, RSV-infected *ager*$^{-/-}$ mice had significantly elevated levels of IFN-I, namely, IFN-α and IFN-β, compared with RSV-infected WT mice. Although plasmacytoid dendritic cells are thought to be the major producers of IFN-I after viral infection, airway epithelial cells are the primary source of IFN-I during RSV infection in vivo [34]. IFN-I are widely recognized as antiviral cytokines that help prevent viral spread; however, their role during RSV infection is unclear. In vitro, it has been shown that RSV interferes with the IFN-I signaling pathway [35], suggesting that these cytokines are an important component of the innate immune response to RSV. However, only low levels of IFN-I have been observed in infected infants, and these levels did not correlate with viral shedding and/or recovery [36]. Although treatment of mice with IFN-α before RSV infection resulted in a small decrease in viral titers [37], IFN-α2a treatment of RSV-infected children did not alter the clinical scores from children treated with the vehicle [38]. Together, these data suggest a limited role for IFN-I in the context of RSV-induced disease, thus making it unlikely that the exaggerated IFN-I response in *ager*$^{-/-}$ mice is responsible for their protection from disease.

We observed elevated levels of sRAGE in BALF from RSV-infected WT mice at 5 days after infection. Unlike in reports from other models, we did not see an up-regulation of membrane RAGE or HMGB-1 in our infection model [16, 17]. There are conflicting views regarding the role of sRAGE in inflammation. Although some studies have shown that sRAGE can induce proinflammatory cytokine secretion and can mediate macrophage and neutrophil migration, survival, and differentiation [39, 40], others have implicated an anti-inflammatory role for sRAGE. Specifically, sRAGE has been shown to block leukocyte recruitment in models of diabetic inflammation [41, 42], peritonitis [33], sepsis [29], arthritis [39], and lipopolysaccharide-induced lung inflammation [43]. These studies argue that sRAGE acts as a decoy receptor to sequester its ligands from

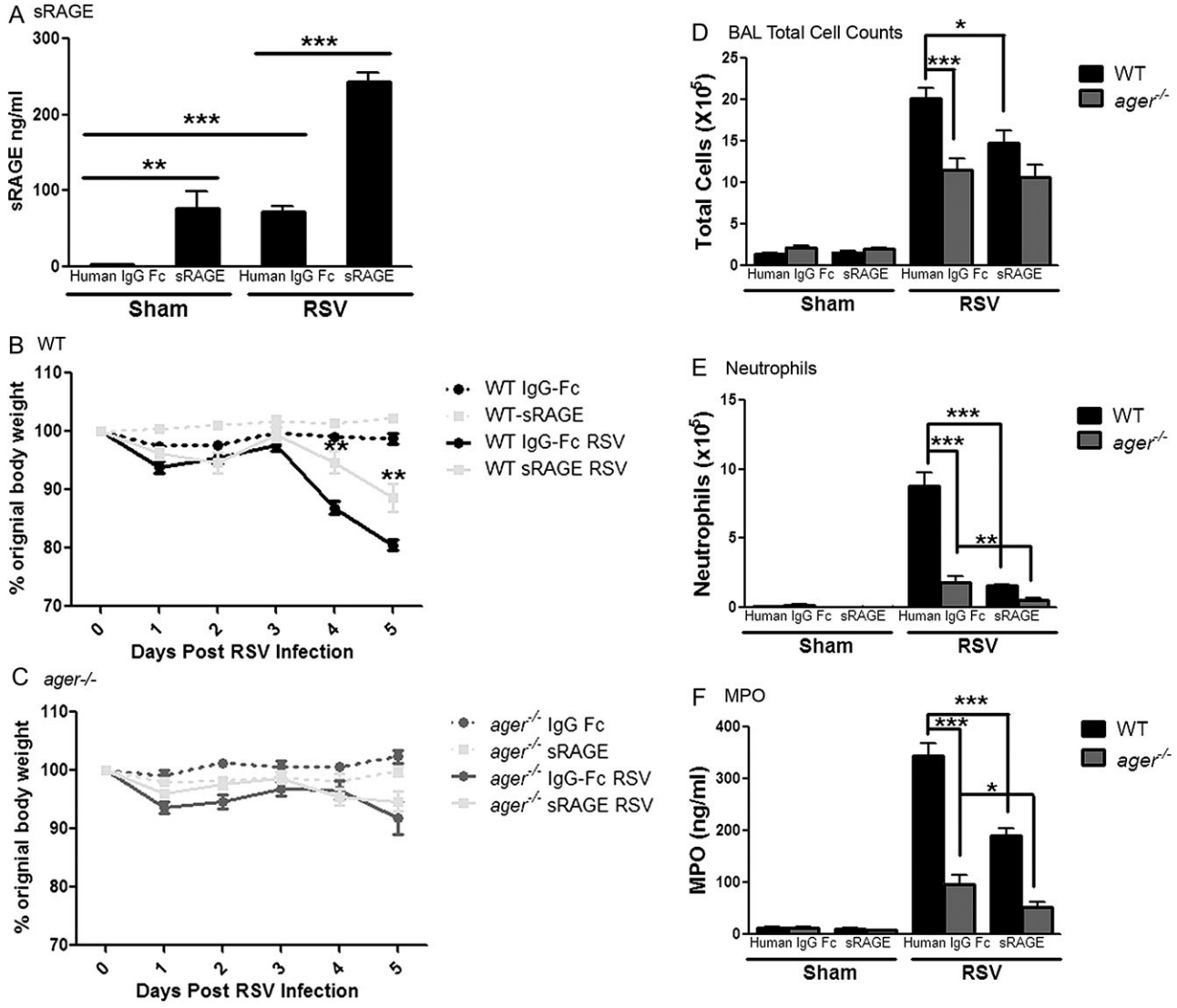

Figure 7. Soluble receptor for advanced glycation end products (sRAGE) protects from parameters of respiratory syncytial virus (RSV)–induced disease. Wild-type (WT) and *ager*$^{-/-}$ mice were sham or RSV infected and administered intranasally with 50 μg of sRAGE or immunoglobulin (Ig) G–Fc at 8 hours and 3 days after infection. *A,* sRAGE-treated RSV-infected mice displayed levels of RAGE that were significantly increased above RAGE levels with RSV infection only. *B–F,* sRAGE protected WT mice (*B*) but not *ager*$^{-/-}$ mice (*C*) from RSV-induced weight loss and bronchoalveolar lavage fluid (BALF) inflammation (*D*), specifically in neutrophils as evidenced by differential counts (*E*) and myeloperoxidase levels (*F*). Data are plotted as mean ± standard error of the mean and represent 2 pooled experiments with 10–16 animals per group. $^{*}P \leq .05$, $^{**}P \leq .01$, $^{***}P \leq .001$.

binding membrane RAGE and inducing a proinflammatory response. A more recent study by Koch et al [44] suggests that sRAGE antagonizes the function of membrane RAGE by physically interacting with membrane RAGE via homotypic interactions and thus preventing the clustering and subsequent signaling through this receptor.

Increases in sRAGE correlate with inflammation and disease in diabetes [45, 46], sepsis [47], and in our model of RSV infection, which lead us to hypothesize that sRAGE was orchestrating the inflammatory response. Therefore, we anticipated that reconstitution of *ager*$^{-/-}$ mice with sRAGE would phenocopy the disease observed in RSV-infected WT mice. However, addition of sRAGE did not exacerbate RSV disease in *ager*$^{-/-}$ mice but, instead, diminished the severity of disease in RSV-infected WT mice. It seems counterintuitive that both RAGE deficiency and treatment of WT mice with exogenous RAGE could be beneficial during RSV infection. Instead, we conclude that there are opposing functions of membrane RAGE and sRAGE. Under normal conditions, RAGE binds its ligands and induces inflammation. However, in the presence of sRAGE, the proinflammatory signaling cascade downstream of membrane RAGE is dampened either by

ligand sequestration or by physical disruption of the signaling complex [44]. Under these circumstances, proinflammatory RAGE signaling would not occur in *ager*$^{-/-}$ mice and would be attenuated with sRAGE treatment of WT mice.

The exact means by which RAGE signaling impacts the pathogenesis of RSV-induced disease are not yet clear. However, our data provide some insights into potential mechanisms. First, RAGE seems to be a negative regulator of IFN-I, and the enhanced IFN-I production observed in *ager*$^{-/-}$ mice may help to limit viral spread. Second, our data implicate RAGE in RSV-induced inflammation, because the absence of RAGE significantly reduced RSV-induced leukocyte recruitment to the lungs. Finally, these data highlight the differences in the functions of membrane and sRAGE. Although signaling via membrane RAGE induces an inflammatory response, interactions between soluble and membrane RAGE and ligand binding to sRAGE seem to be mechanisms by which the host can down-modulate inflammation.

Notes

Financial support. This work was supported by MedImmune, LLC.

Potential conflicts of interest. All authors: No reported conflicts.

All authors have submitted the ICMJE Form for Disclosure of Potential Conflicts of Interest. Conflicts that the editors consider relevant to the content of the manuscript have been disclosed.

References

1. Perez-Yarza EG, Moreno A, Lazaro P, Mejias A, Ramilo O. The association between respiratory syncytial virus infection and the development of childhood asthma: a systematic review of the literature. Pediatr Infect Dis J **2007**; 26:733–9.
2. Hall CB, Weinberg GA, Iwane MK, et al. The burden of respiratory syncytial virus infection in young children. N Engl J Med **2009**; 360: 588–98.
3. Ramirez JA. RSV infection in the adult population. Manag Care **2008**; 17(11 Suppl 12):13–15, discussion.
4. The World Health Organization. The global burden of disease. Geneva, Switzerland: WHO Press, **2004**: 23.
5. Ko FW, Ip M, Chan PK, et al. Viral etiology of acute exacerbations of COPD in Hong Kong. Chest **2007**; 132:900–8.
6. Ko FW, Ip M, Chan PK, et al. A 1-year prospective study of the infectious etiology in patients hospitalized with acute exacerbations of COPD. Chest **2007**; 131:44–52.
7. Cameron RJ, de WD, Welsh TN, Ferguson J, Grissell TV, Rye PJ. Virus infection in exacerbations of chronic obstructive pulmonary disease requiring ventilation. Intensive Care Med **2006**; 32:1022–9.
8. Camargo CA Jr, Ginde AA, Clark S, Cartwright CP, Falsey AR, Niewoehner DE. Viral pathogens in acute exacerbations of chronic obstructive pulmonary disease. Intern Emerg Med **2008**; 3:355–9.
9. Seemungal T, Harper-Owen R, Bhowmik A, et al. Respiratory viruses, symptoms, and inflammatory markers in acute exacerbations and stable chronic obstructive pulmonary disease. Am J Respir Crit Care Med **2001**; 164:1618–23.
10. Borg I, Rohde G, Loseke S, et al. Evaluation of a quantitative real-time PCR for the detection of respiratory syncytial virus in pulmonary diseases. Eur Respir J **2003**; 21:944–51.
11. Wilkinson TM, Donaldson GC, Johnston SL, Openshaw PJ, Wedzicha JA. Respiratory syncytial virus, airway inflammation, and FEV1 decline in patients with chronic obstructive pulmonary disease. Am J Respir Crit Care Med **2006**; 173:871–6.
12. Santilli F, Vazzana N, Bucciarelli LG, Davi G. Soluble forms of RAGE in human diseases: clinical and therapeutical implications. Curr Med Chem **2009**; 16:940–52.
13. Sims GP, Rowe DC, Rietdijk ST, Herbst R, Coyle AJ. HMGB1 and RAGE in inflammation and cancer. Annu Rev Immunol **2010**; 28: 367–88.
14. Fehrenbach H, Kasper M, Tschernig T, Shearman MS, Schuh D, Muller M. Receptor for advanced glycation endproducts (RAGE) exhibits highly differential cellular and subcellular localisation in rat and human lung. Cell Mol Biol (Noisy-le-grand) **1998**; 44:1147–57.
15. Katsuoka F, Kawakami Y, Arai T, et al. Type II alveolar epithelial cells in lung express receptor for advanced glycation end products (RAGE) gene. Biochem Biophys Res Commun **1997**; 238:512–16.
16. van Zoelen MA, van der Sluijs KF, Achouiti A, et al. Receptor for advanced glycation end products is detrimental during influenza A virus pneumonia. Virology **2009**; 391:265–73.
17. van Zoelen MA, Schouten M, de Vos AF, et al. The receptor for advanced glycation end products impairs host defense in pneumococcal pneumonia. J Immunol **2009**; 182:4349–56.
18. Miller AL, Bowlin TL, Lukacs NW. Respiratory syncytial virus-induced chemokine production: linking viral replication to chemokine production in vitro and in vivo. J Infect Dis **2004**; 189:1419–30.
19. Tekkanat KK, Maassab HF, Cho DS, et al. IL-13-induced airway hyperreactivity during respiratory syncytial virus infection is STAT6 dependent. J Immunol **2001**; 166:3542–8.
20. Bueno SM, Gonzalez PA, Cautivo KM, et al. Protective T cell immunity against respiratory syncytial virus is efficiently induced by recombinant BCG. Proc Natl Acad Sci U S A **2008**; 105:20822–7.
21. Fulton RB, Meyerholz DK, Varga SM. Foxp3+ CD4 regulatory T cells limit pulmonary immunopathology by modulating the CD8 T cell response during respiratory syncytial virus infection. J Immunol **2010**; 185:2382–92.
22. Hashimoto K, Mori S, Hashimoto Y, et al. DSCG reduces RSV-induced illness in RSV-infected mice. J Med Virol **2009**; 81:354–61.
23. Hayes PJ, Scott R, Wheeler J. In vivo production of tumour necrosis factor-alpha and interleukin-6 in BALB/c mice inoculated intranasally with a high dose of respiratory syncytial virus. J Med Virol **1994**; 42: 323–9.
24. Lee DC, Harker JA, Tregoning JS, et al. CD25+ natural regulatory T cells are critical in limiting innate and adaptive immunity and resolving disease following respiratory syncytial virus infection. J Virol **2010**; 84:8790–8.
25. Zhang W, Choi Y, Haynes LM, et al. Vaccination to induce antibodies blocking the CX3C-CX3CR1 interaction of respiratory syncytial virus G protein reduces pulmonary inflammation and virus replication in mice. J Virol **2010**; 84:1148–57.
26. Graham BS, Bunton LA, Wright PF, Karzon DT. Role of T lymphocyte subsets in the pathogenesis of primary infection and rechallenge with respiratory syncytial virus in mice. J Clin Invest **1991**; 88:1026–33.
27. Tregoning JS, Pribul PK, Pennycook AM, et al. The chemokine MIP1alpha/CCL3 determines pathology in primary RSV infection by regulating the balance of T cell populations in the murine lung. PLoS One **2010**; 5:e9381.
28. Graham BS, Perkins MD, Wright PF, Karzon DT. Primary respiratory syncytial virus infection in mice. J Med Virol **1988**; 26:153–62.
29. Liliensiek B, Weigand MA, Bierhaus A, et al. Receptor for advanced glycation end products (RAGE) regulates sepsis but not the adaptive immune response. J Clin Invest **2004**; 113:1641–50.
30. Lutterloh EC, Opal SM, Pittman DD, et al. Inhibition of the RAGE products increases survival in experimental models of severe sepsis and systemic infection. Crit Care **2007**; 11:R122.
31. Johnson TR, Hong S, Van KL, Koezuka Y, Graham BS. NK T cells contribute to expansion of $CD8^+$ T cells and amplification of antiviral immune responses to respiratory syncytial virus. J Virol **2002**; 76: 4294–303.

32. Frommhold D, Kamphues A, Hepper I, et al. RAGE and ICAM-1 cooperate in mediating leukocyte recruitment during acute inflammation in vivo. Blood **2010**; 116:841–9.
33. Chavakis T, Bierhaus A, Al-Fakhri N, et al. The pattern recognition receptor (RAGE) is a counterreceptor for leukocyte integrins: a novel pathway for inflammatory cell recruitment. J Exp Med **2003**; 198: 1507–15.
34. Jewell NA, Vaghefi N, Mertz SE, et al. Differential type I interferon induction by respiratory syncytial virus and influenza a virus in vivo. J Virol **2007**; 81:9790–800.
35. Ramaswamy M, Shi L, Monick MM, Hunninghake GW, Look DC. Specific inhibition of type I interferon signal transduction by respiratory syncytial virus. Am J Respir Cell Mol Biol **2004**; 30:893–900.
36. McIntosh K. Interferon in nasal secretions from infants with viral respiratory tract infections. J Pediatr **1978**; 93:33–6.
37. Guerrero-Plata A, Baron S, Poast JS, Adegboyega PA, Casola A, Garofalo RP. Activity and regulation of alpha interferon in respiratory syncytial virus and human metapneumovirus experimental infections. J Virol **2005**; 79:10190–9.
38. Sung RY, Yin J, Oppenheimer SJ, Tam JS, Lau J. Treatment of respiratory syncytial virus infection with recombinant interferon alfa-2a. Arch Dis Child **1993**; 69:440–2.
39. Pullerits R, Brisslert M, Jonsson IM, Tarkowski A. Soluble receptor for advanced glycation end products triggers a proinflammatory cytokine cascade via beta2 integrin Mac-1. Arthritis Rheum **2006**; 54:3898–907.
40. Wang Y, Wang H, Piper MG, et al. sRAGE induces human monocyte survival and differentiation. J Immunol **2010**; 185:1822–35.
41. Bucciarelli LG, Wendt T, Qu W, et al. RAGE blockade stabilizes established atherosclerosis in diabetic apolipoprotein E-null mice. Circulation **2002**; 106:2827–35.
42. Kislinger T, Tanji N, Wendt T, et al. Receptor for advanced glycation end products mediates inflammation and enhanced expression of tissue factor in vasculature of diabetic apolipoprotein E-null mice. Arterioscler Thromb Vasc Biol **2001**; 21:905–10.
43. Zhang H, Tasaka S, Shiraishi Y, et al. Role of soluble receptor for advanced glycation end products on endotoxin-induced lung injury. Am J Respir Crit Care Med **2008**; 178:356–62.
44. Koch M, Chitayat S, Dattilo BM, et al. Structural basis for ligand recognition and activation of RAGE. Structure **2010**; 18:1342–52.
45. Nakamura K, Yamagishi S, Adachi H, et al. Elevation of soluble form of receptor for advanced glycation end products (sRAGE) in diabetic subjects with coronary artery disease. Diabetes Metab Res Rev **2007**; 23:368–71.
46. Nin JW, Ferreira I, Schalkwijk CG, et al. Levels of soluble receptor for AGE are cross-sectionally associated with cardiovascular disease in type 1 diabetes, and this association is partially mediated by endothelial and renal dysfunction and by low-grade inflammation: the EURODIAB Prospective Complications Study. Diabetologia **2009**; 52:705–14.
47. Bopp C, Hofer S, Weitz J, et al. sRAGE is elevated in septic patients and associated with patients outcome. J Surg Res **2008**; 147:79–83.